Acta Geod Geophys (2016) 51:619–641
DOI 10.1007/s40328-016-0159-3

Assessment of numerical integration methods in the context of low Earth orbits and inter-satellite observation analysis

Thomas D. Papanikolaou[1] · **Dimitrios Tsoulis**[1]

Received: 7 September 2015 / Accepted: 6 January 2016 / Published online: 26 January 2016

Abstract The integration of differential equations is a fundamental tool in the problem of orbit determination. In the present study, we focus on the accuracy assessment of numerical integrators in what refers to the categories of single-step and multistep methods. The investigation is performed in the frame of current satellite gravity missions i.e. Gravity Recovery and Climate Experiment (GRACE) and Gravity Field and steady-state Ocean Circulation Explorer (GOCE). Precise orbit determination is required at the level of a few cm in order to satisfy the primary missions' scope which is the rigorous modelling of the Earth's gravity field. Therefore, the orbit integration errors are critical for these low earth orbiters. As the result of different schemes of numerical integration is strongly affected by the forces acting on the satellites, various validation tests are performed for their accuracy assessment. The performance of the numerical methods is tested in the analysis of Keplerian orbits as well as in real dynamic orbit determination of GRACE and GOCE satellites by taking into account their sophisticated observation techniques and orbit design. Numerical investigation is performed in a wide range of the fundamental integrators' parameters i.e. the integration step and the order of the multistep methods.

Keywords Numerical integration · Orbit determination · Runge–Kutta–Nyström · Multistep methods · Satellite gravity missions

✉ Thomas D. Papanikolaou
thomas.papanikolaou@ga.gov.au; tp@thomaspap.com

Dimitrios Tsoulis
tsoulis@auth.gr;
http://users.auth.gr/tsoulis

[1] Department of Geodesy and Surveying, Aristotle University of Thessaloniki, Thessaloniki, Greece

1 Introduction

Integration of differential equations is one of the underlying tools in the problem of orbit determination. Numerical integration methods are widely used for the orbit computations of artificial satellites and solar system bodies. The numerical integrators react differently for each orbit type e.g. low earth orbit (LEO), medium earth orbit (MEO), as they are strongly affected by the orbit dynamics. Thus, quality control of the numerical methods is required for each individual orbit analysis (Montenbruck and Gill 2000) prior to the operational use in the procedure of orbit determination products. A variety of tests for the comparison of numerical integrators through orbit analysis can be found in Hull et al. (1972), Fox (1984), Montenbruck (1992), Somodi and Földvary (2011). One commonly used test in the corresponding literature is the numerical analysis of Keplerian orbits. This kind of analysis is well discussed in Sect. 3 where it is applied for the cases of LEO and MEO orbits.

Precise orbit determination is a major requirement in the case of several satellite missions, namely satellite altimetry and gravimetric missions. The mathematical connection between the satellite motion and the gravity field is a key link in the frame of dedicated satellite gravity missions, especially Gravity Recovery and Climate Experiment (GRACE) and Gravity Field and steady-state Ocean Circulation Explorer (GOCE) missions (Tapley et al. 2004; ESA 1999; Floberghagen et al. 2011), whose measurement principles require a precise orbit determination at the level of a few cm (Förste et al. 2008; Pail et al. 2011). The space-borne techniques of the two missions have generated extended numerical investigations in the Earth's gravity field modelling as well as into the satellite orbit determination (Xu 2008a; Ilk et al. 2008; Svehla and Rothacher 2003; Bobojć and Drożyner 2003; Beutler et al. 2010a; Kang et al. 2006a, b; Bock et al. 2011).

In the case of these satellite missions, rigorous treatment of the perturbations and the observations errors is required in order to capture the measured Earth's gravity signal at the orbital altitude. In such a case, precise orbit determination is required at the level of a few cm for satisfying the major missions' goal, i.e. the rigorous modelling of the Earth's gravity field. Therefore, the orbit integration errors may be critical for such low Earth orbiters.

The present study aims to the comparison and accuracy assessment of numerical integrators such as single-step and multistep integration methods. Apart from the comparison of the used numerical methods, the current numerical investigation focuses on the fundamental parameters of the integrators i.e. the integration step-size and the order of the multistep methods. The orbit computations are repeated for a wide range of these input parameters. Moreover, we examine the required computation time which forms an additional criterion for the selection of a specific integration method and the values of the considered parameters.

Here, we implement the comparison between the analytical solution and the numerical integration of Keplerian orbits, which is known as the two-body problem test (Montenbruck 1992; Fox 1984; Hull et al. 1972). Nevertheless, this classical test does not satisfy a real orbit scenario. Since the numerical methods are sensitive to the satellite dynamics, we test the performance of the methods in dynamic orbit determination by using real satellite data. The real orbit analysis is performed by considering the sophisticated observation techniques and the orbit design of GRACE and GOCE missions.

The GRACE mission is, since 2002, implementing the concept of low–low satellite-to-satellite tracking (SST) through a K-band ranging (KBR) system that provides μm level

accuracy (Kim and Tapley 2002). The current approach, in evaluating the integrators accuracy based on rigorous KBR data analysis, may also be found useful to investigations of a future satellite gravity mission that is under study (Loomis et al. 2012; Panet et al. 2013; Elsaka et al. 2014). The future mission's concept is oriented in intersatellite ranging observations with higher requirements in accuracy standards by at least a few orders of magnitude (Loomis et al. 2012; Sheard et al. 2012) and it is designed by considering the achievements as well as the limitations of the measurements principles of the GRACE and GOCE missions.

2 Orbit integrators

The basic mathematical tool for the description of a satellite orbit is given by Newton's second law

$$m\ddot{\mathbf{r}} = \mathbf{F}, \tag{1}$$

where $\ddot{\mathbf{r}}$ denotes the acceleration vector, m the satellite's mass and $\mathbf{F}$ the sum of all forces acting on the satellite, which includes both gravitational and non-gravitational effects.

The equation of motion (1) is a second-order differential equation and its solution requires the application of some kind of an integration method. This can be performed by analytical methods (Brouwer 1959; Kozai 1959; Wnuk 1999) or numerical integration methods (Seeber 2003; Montenbruck and Gill 2000). The analytical approach leads to a closed formula for the solution. Nevertheless, in case of strong perturbations, the analytical solution becomes quite elaborate. Rigorous approaches in analytical orbit determination are given by Xu (2008b), Cui (1997), Cui and Lelgemann (1995), (2000). The numerical integration methods provide high accuracy and are characterized by their simplicity in comparison with the analytical methods in orbit problems. Therefore, the numerical approach is used widely in the fields of astrodynamics and celestial mechanics.

The majority of numerical integrators for Eq. (1) are formulated as first-order differential equation solvers. The equation of motion may be written in a suitable form for this purpose as follows

$$\dot{\mathbf{y}} = \mathbf{f}(t, \mathbf{y}) = \begin{pmatrix} \dot{\mathbf{r}} \\ \mathbf{F}(t, \mathbf{r}, \dot{\mathbf{r}})/m \end{pmatrix}, \tag{2}$$

where $\mathbf{r}$ and $\dot{\mathbf{r}}$ are the position and velocity vectors respectively.

The state vector consists of the position and velocity vectors and is denoted by

$$\mathbf{y} = \begin{pmatrix} \mathbf{r} \\ \dot{\mathbf{r}} \end{pmatrix}. \tag{3}$$

In order to apply a numerical integration method, the initial values of the state vector are required as well as the acceleration which is computed at every epoch according to a known force model, optionally complemented by measurements gathered by the on-board accelerometer. Furthermore, suitable values of the integration step size and order are required. Small values for the integration step size may lead to low local truncation errors. Nevertheless, this is satisfactory only for a short period of integration time while for longer orbit arcs the round off errors and the computation effort increase rapidly. According to these criteria, optimum values are needed in order to achieve a precise solution in a practical amount of computational time. The selection of these values is an objective to be

investigated for each individual problem of orbit determination (Montenbruck and Gill 2000).

In the present analysis, we apply efficient numerical integration methods which are classified in the categories of Runge–Kutta–Nyström (RKN) and multistep methods. In particular, the following methods have been implemented in our software

- RKN7(6)-8: 7th order RKN method developed by Dormand and Prince (1978)
- RKN6(4)-6FD: 6th order RKN method proposed by Dormand and Prince (1987)
- Adams–Bashforth-Moulton
- Gauss-Jackson
- Gauss-Jackson (predictor–corrector)

The RKN7(6)-8 and RKN6(4)-6FD belong to the category of the Runge–Kutta–Nyström methods while the rest of the listed methods refer to the general category of multistep methods. The basic mathematical formulas for the aforementioned numerical methods are described here while an extended description is given by Montenbruck and Gill (2000), Xu (2008b) and Beutler (2005).

2.1 Runge–Kutta–Nyström methods

The family of Runge–Kutta–Nyström numerical methods has the advantage that it is especially designed for the direct integration of second order differential equations. A special set of RKN methods may be applied in the case the force model is independent from the velocity vector and the acceleration vector may be written as

$$\mathbf{a}(t,\mathbf{r}) = \mathbf{F}(t,\mathbf{r})/m, \tag{4}$$

where $\mathbf{a}$ is the acceleration vector.

Such RKN methods are described by the equations

$$\begin{aligned}
\mathbf{k_i} &= \mathbf{a}\left(t_0 + c_i h,\ \mathbf{r_0} + c_i h \boldsymbol{\upsilon_0} + h^2 \sum_{j=0}^{i-1} a_{ij}\mathbf{k_j}\right)\\
\hat{\mathbf{r}}(t_0+h) &= \mathbf{r_0} + h\boldsymbol{\upsilon_0} + h^2 \sum_{i=0}^{s} \hat{b}_i \mathbf{k_i}\\
\hat{\boldsymbol{\upsilon}}(t_0+h) &= \boldsymbol{\upsilon_0} + h \sum_{i=0}^{s} \hat{\dot{b}}_i \mathbf{k_i}.
\end{aligned} \tag{5}$$

The variables t_0, $\mathbf{r}_0$, $\boldsymbol{\upsilon_0}$ refer to the initial conditions i.e. the reference epoch and the position and velocity vectors components respectively, while the variable h denotes the integration step.

The coefficients c_i, a_{ij}, k_i, b_i, $\hat{b}_i$, $\hat{\dot{b}}_i$ describe the specific RKN method. These coefficients are computed for the RKN7(6)-8 and RKN6(4)-6FD methods by Dormand and Prince (1978) and Dormand and Prince (1987) correspondingly.

The $\mathbf{k_i}$ components are the function evaluations that are being computed for every integration step. The variable s denotes the number of these evaluations and it is defined by each specific RKN method.

Vectors $\hat{\mathbf{r}}$, $\hat{\upsilon}$ represent the integration's solution for the position and velocity vector respectively at the end of the integration step i.e. the epoch t_0+h.

2.2 Adams–Bashforth-Moulton method

The basic principle of the multistep methods relies on the replacement of the equation of motion's integrand by an equivalent polynomial

$$\mathbf{y}(t_{i+1}) = \mathbf{y}(t_i) + \int_{t_i}^{t_i+h} \mathbf{f}(t,\ \mathrm{y}(t))dt \simeq \mathbf{y}(t_i) + \int_{t_i}^{t_i+h} p(t)dt \tag{6}$$

The polynomial is computed by the fitting of $p(t)$ to some of the values of the function $\mathbf{f}(t, \mathbf{y}(t))$ at previous times, where the state vector is known. The known values of the state vector at the initial epochs can be determined by a Runge–Kutta method which is used only to determine the initial values at the first some epochs where the number of epochs depends on the selected order of the polynomial $p(t)$.

The Adams–Bashforth algorithm makes use of the equation

$$\mathrm{p}_m^i(t) = \mathrm{p}_m^i(t_i + \sigma h) = \sum_{j=0}^{m-1} (-1)^j \binom{-\sigma}{j} \nabla^j \mathbf{f_i} \tag{7}$$

for the evaluation of the polynomial of arbitrary order m where $\sigma = (t_{i+1} - t_i)/h$. The polynomial p_m^i interpolates $m + 1$ points of the function $\mathbf{f_i}$ at the past previous points.

The binomial coefficient is computed as

$$\binom{-\sigma}{j} = \frac{(-\sigma)(-\sigma - 1)\ldots(-\sigma - j + 1)}{j!}, \quad j > 0 \tag{8}$$

and it is equal to 1 for $j = 0$.

The backward differences are defined as

$$\begin{aligned} \nabla^0 f_i &= f_i \\ \nabla f_i &= f_i - f_{i-1} \\ \nabla^n f_i &= \nabla^{n-1} f_i - \nabla^{n-1} f_{i-1} \end{aligned} \tag{9}$$

The solution is obtained by the equation

$$\mathbf{y}(t_{i+1}) = \mathbf{y}(t_i) + h \sum_{j=0}^{m-1} \gamma_j \nabla^j \mathbf{f_i}, \tag{10}$$

where the coefficients γ are computed by the equation

$$\gamma_j = 1 - \sum_{k=0}^{j-1} \frac{1}{j + 1 - k} \gamma_k, \tag{11}$$

and γ_0 is equal to 1.

The values of the integration step h and the order m are the critical parameters that have to be selected for the implementation of the numerical method.

The Adams–Moulton formula makes use of the previous function values and one additional function value at the integration epoch i.e. next epoch. In this case, the corresponding polynomial is described by the equation

$$\mathrm{p}_m^{i+1}(t) = \mathrm{p}_m^{i+1}(t_i + \sigma h) = \sum_{j=0}^{m-1} (-1)^j \binom{-\sigma + 1}{j} \nabla^j \mathbf{f_{i+1}}. \tag{12}$$

The integration's solution is obtained by the equation

$$\mathbf{y}(t_{i+1}) = \mathbf{y}(t_i) + h \sum_{j=0}^{m-1} \gamma_j^* \nabla^j \mathbf{f_{i+1}}, \tag{13}$$

where

$$\gamma_j^* = -\sum_{k=0}^{j-1} \frac{1}{j+1-k} \gamma_k^*, \tag{14}$$

and γ_0^* is equal to 1.

Equation (13) is dependent of the **f** function's value at the integration epoch which is not a known value since the position and velocity vector is not known at this epoch. Therefore, the Adams–Moulton cannot provide a solution by itself, but can deliver a prediction. It is combined with the Adams–Bashforth method, which corrects the estimate of the Adams–Moulton method. Such a method is referred to as predictor–corrector algorithm, which is described in Montenbruck and Gill (2000) and Berry and Healy (2004). The method referred in this study as Adams–Bashforth-Moulton method is applied for this predictor–corrector approach.

2.3 Gauss-Jackson methods

The Gauss-Jackson methods are especially designed for the direct integration of 2nd order differential equations. Their formula is defined by the equations

$$\mathbf{r_{i+1}} = h^2 \sum_{j=0}^{m+1} \delta_j \nabla^{j-2} \mathbf{a_i}, \tag{15}$$

$$\boldsymbol{\upsilon}_{\mathbf{i+1}} = h \sum_{j=0}^{m} \gamma_j \nabla^{j-1} \mathbf{a_i}, \tag{16}$$

where the coefficients δ_j are computed according to the equation

$$\delta_j = (1-j)\gamma_j^*. \tag{17}$$

The approach of the predictor–corrector algorithm may also be implemented for the Gauss-Jackson formulas and the final solution is derived by the equations

$$\mathbf{r_{i+1}} = h^2 \sum_{j=0}^{m+1} \delta_j^* \nabla^{j-2} \mathbf{a_{i+1}}, \tag{18}$$

$$\boldsymbol{\upsilon}_{\mathbf{i+1}} = h \sum_{j=0}^{m} \gamma_j^* \nabla^{j-1} \mathbf{a_{i+1}}, \tag{19}$$

where the coefficients δ_j^* are computed as follows

$$\delta_j^* = \delta_j - \delta_{j-1}. \tag{20}$$

The first and second sum are defined as

$$\begin{aligned} \mathbf{a_i} &= \nabla^{-1}\mathbf{a}_i - \nabla^{-1}\mathbf{a}_{i-1}, \\ \nabla^{-1}\mathbf{a}_i &= \nabla^{-2}\mathbf{a}_i - \nabla^{-2}\mathbf{a}_{i-1}, \end{aligned} \tag{21}$$

and the initial values for the backward differences are obtained as follows

$$\begin{aligned} \nabla^{-1}\mathbf{a_0} &= \frac{\boldsymbol{\upsilon_0}}{h} - \sum_{j=1}^{m} \gamma_j^* \nabla^{j-1}\mathbf{a_0}, \\ \nabla^{-2}\mathbf{a_0} &= \frac{\mathbf{r_0}}{h^2} - \sum_{j=1}^{m+1} \delta_j^* \nabla^{j-2}\mathbf{a_0}. \end{aligned} \tag{22}$$

3 Keplerian orbit analysis

A straightforward test for the assessment of numerical integration methods is to apply them to a set of differential equations which are integrable by analytical methods so that the solution is given by closed mathematical formulas. The comparison among the analytical and numerical solution defines an absolute control for the accuracy of the numerical integrators. This kind of test indicates the errors that come from the numerical integration according to the selected integration step and order. The Keplerian orbit, which is the solution to the two-body problem where only the gravitational attraction resulting from one

Table 1 Orbit parameterization for the integration of Keplerian orbits

Orbit integration parameters			
Orbit type	LEO (GOCE)		MEO (GIOVE-A)
Orbital altitude	255 km		23,220 km
Arc length		24 h	
Integrators		RKN7(6)-8	
		RKN6(4)-6FD	
		Adams–Bashforth-Moulton	
		Gauss-Jackson	
		Gauss-Jackson (pc)	
Start integrator		RKN7(6)-8	
Integration step	10–250 s		2–30 min
Order		2–16	
Initial conditions			
Semi-major axis	6633 km		29,600 km
Eccentricity	0.001		0.009
Inclination	96°		56°
Ascending node	162°		150°
Argument perigee	45°		340°
Mean anomaly		0	

point-mass is considered, is a suitable test for this purpose. The analytical formulas for Keplerian orbits can be found in various articles, such as Kaula (1966), Montenbruck and Gill (2000), Seeber (2003) and Xu (2008b), Casotto (1993).

The aforementioned approach has been implemented here for two different scenarios of Keplerian orbits i.e. low earth orbit (LEO) and medium earth orbit (MEO) orbit types. The selected orbit characteristics for these two cases are roughly based on the mean Keplerian elements of GOCE and Galileo in-orbit validation element (GIOVE-A) satellite orbits, respectively (Table 1). Preliminary results of this approach have been reported in Tsoulis et al. (2011).

By considering the values of the Kepler elements listed in Table 1 as known initial conditions, the orbit integration is performed and then, the comparison among the numerical solution and the constant Keplerian elements is applied. Orbit computations have been carried out for daily orbit arcs. The integration step, in the presented results, varies in the ranges of 10–250 s and 2–30 min for LEO and MEO types respectively. Lower values of the integration step lead to orbit differences varying in the same order of magnitude. The orbit integration has been repeated by modifying the integration step size each time with an interval of 1 s within the step range. The order of multistep methods has been selected in the range of 2–16. In order to initiate the numerical integration for the first steps of the multi-step methods, as it is a standard requirement, the RKN7(6)-8 method has been applied as a start integrator.

The considered orbit parameters are shown in Table 1 while the orbit comparisons are drawn in Figs. 1 and 2. The order of multistep methods in these figures has been set equal to 8.

The numerical comparison in all results is represented by the root mean square (RMS) of the orbit differences for the Keplerian elements among the numerical solution and the analytical approach i.e. the constant Kepler elements.

In the LEO case, computations for orders varying from 7 to 16 show similar orbit differences while in the case of MEO this is valid for orders varying from 8 to 14. Beyond these limits, higher and significant orbit differences have been obtained. The RMS variations for the elements of inclination and argument of the ascending node present negligible values, at the level of 10^{-14}–10^{-10} degrees, for all of the integration methods within the full range of the varying parameters i.e. the integration step and the order of the multistep methods. According to the orbit computations, the Runge–Kutta–Nyström methods show high numerical stability while the lowest RMS values have been obtained for the RKN7(6)-8 method.

In the case of multistep methods, the RMS variations remain at a low level, e.g. sub-mm in the semi-major axis differences, for values of the integration step up to 30 s and 5 min for LEO and MEO orbit type correspondingly. Beyond these limits detectable discrepancies occur that may exceed the meter level for the higher selected integration step values.

The numerical analysis of Keplerian orbits is demonstrated as a valuable tool for monitoring the numerical behaviour of orbit integrators. It is shown that preferable values, by means of accuracy, of the integration step may vary in the ranges of 10–20 s and 2–3 min for the cases of LEO and MEO orbits respectively. In the case of the Runge–Kutta–Nyström methods the upper limits may be higher since these numerical algorithms have been found to be numerically stable and lead to lower RMS results in comparison with the multistep methods.

However, this test based on Keplerian orbits may be considered as a preliminary assessment of the numerical integration methods. Therefore, an in-depth real orbit analysis, which is affected by the natural orbit perturbations, would be able to indicate optimum

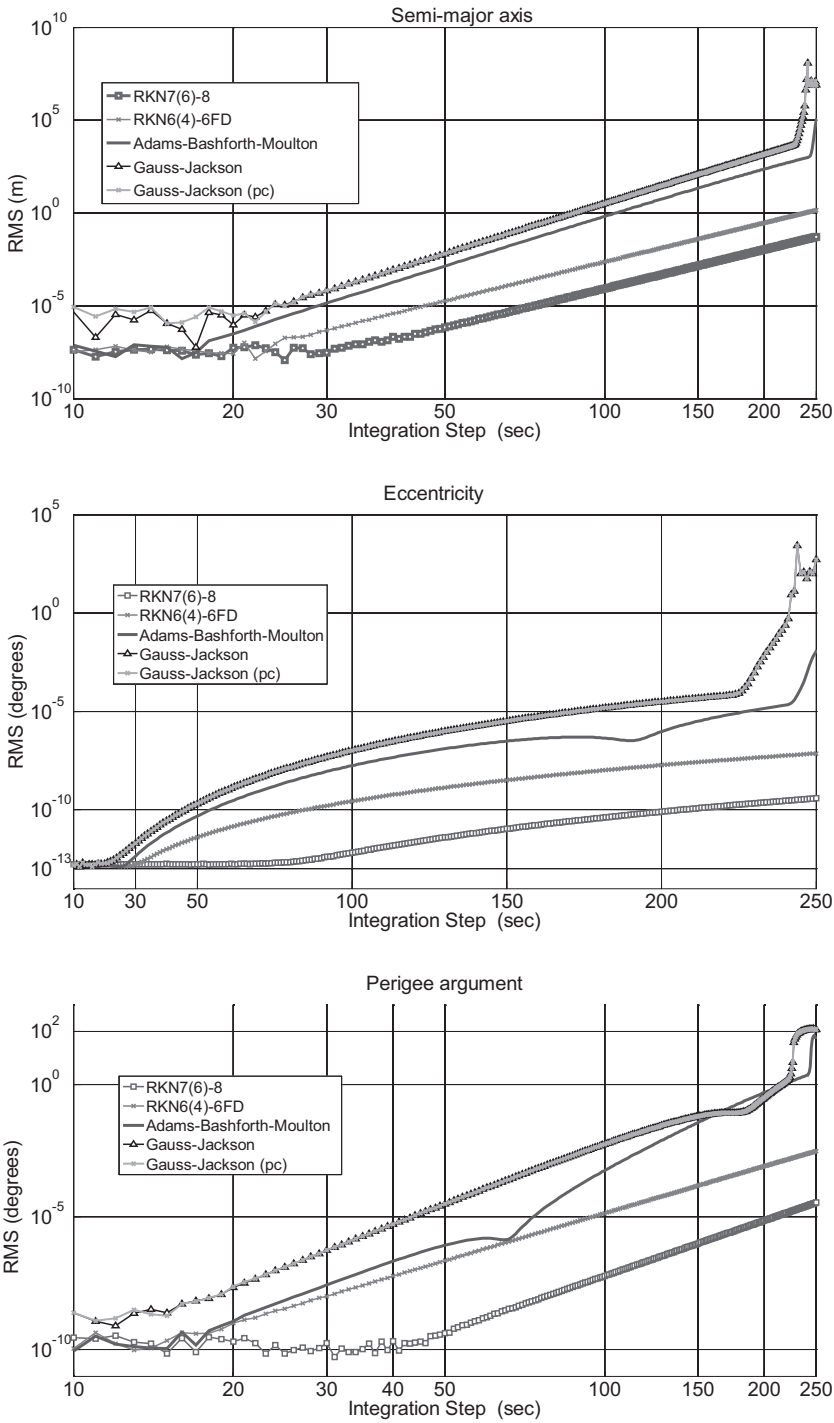

Fig. 1 RMS variances of Keplerian orbit differences between analytical and numerical solution for LEO type. The order of the multistep methods has been set equal to 8

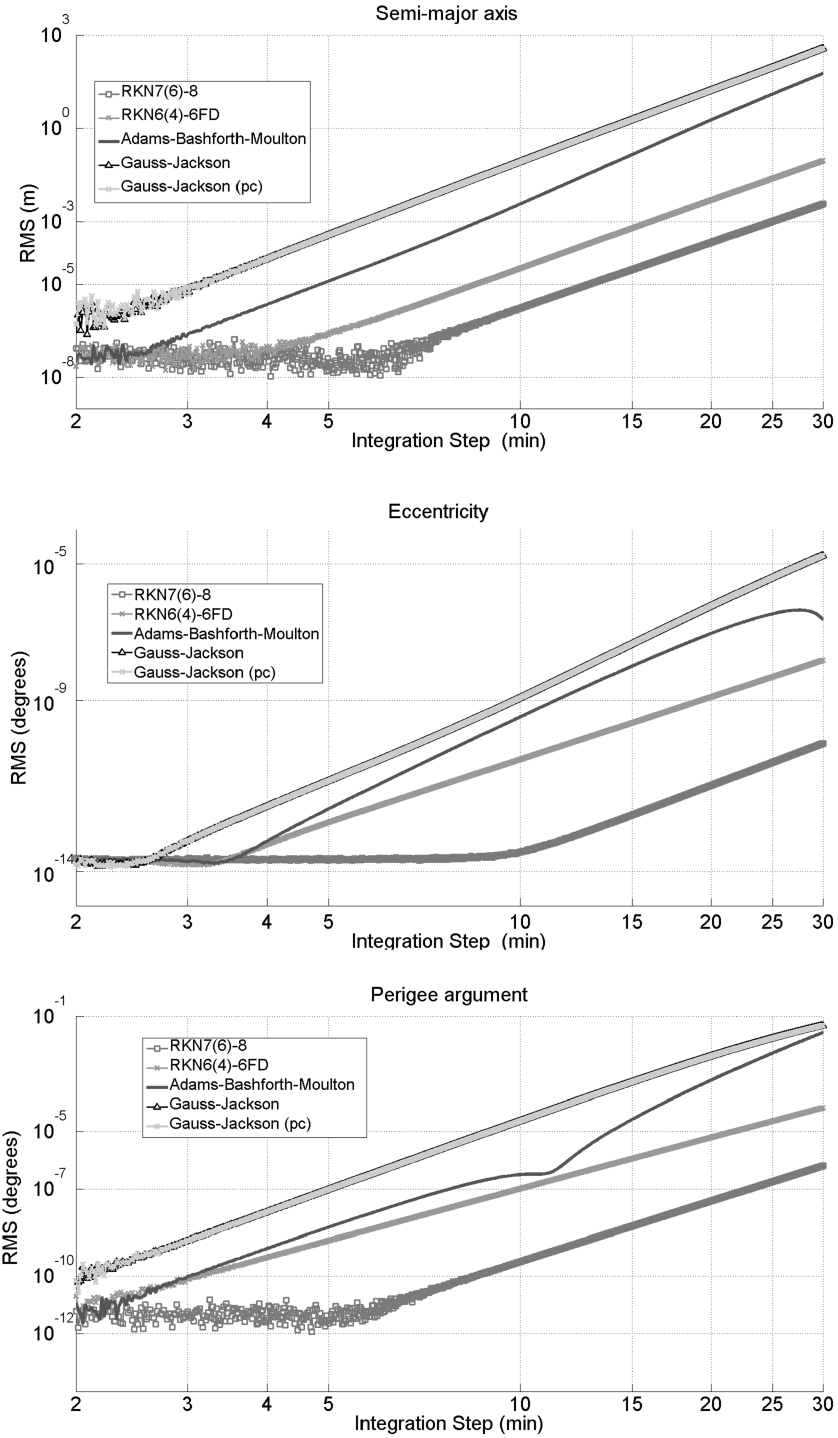

Fig. 2 RMS variances of Keplerian orbit differences between analytical and numerical solution for MEO type. The order of the multistep methods has been set equal to 8

parameters of the numerical integration algorithms. Thus, we perform such an orbit analysis in the following section.

4 Dynamic orbit determination

In the frame of estimation theory, the problem of orbit determination may be considered as a generalized adjustment problem with several required estimated parameters. The minimum set of these unknown parameters usually refers to the initial position and velocity vector. Under these conditions, the orbit determination problem is regarded as an initial values problem.

The variational equations define a special set of differential equations that is formed by the partial derivatives of the equation of motion. The equation of motion has to be integrated simultaneously with the variational equations (Montenbruck and Gill 2000). The solution of this overall system of differential equations together with the satellite observations are used in the orbit adjustment procedure for the estimation of a set of orbit parameters (Beutler 2005). The accuracy of the estimated parameters is strongly dependent on the completeness and representability of the force model and the quality of the observations.

In the present analysis, the least-squares method has been applied for the estimation procedure. The estimated parameters include the initial position and velocity vectors of the satellite and additional parameters of empirical effects. In the current study, the bias and one cycle per revolution accelerations (Luthcke et al. 2003; Colombo 1986) are considered as empirical parameters. The kinematic positions that are obtained from the precise kinematic orbit determination (Svehla and Rothacher 2003, 2005) are used here as observations. This is an equivalent but simplified approach to the use of the original GPS observations (Beutler et al. 2010b).

4.1 GOCE and GRACE orbit analysis

The concept of dynamic orbit determination applied to the GOCE and GRACE data is the one discussed by Papanikolaou and Tsoulis (2014). Our software has been developed by Papanikolaou (2012) in Matlab and C (minor part) while the current version implements the dynamic orbit modelling as summarized in Table 2. The performed computations consider the Matlab double precision (64 bits) floating point numerical representation.

Satellite data from GRACE and GOCE missions require a suitable preprocessing prior to their further analysis for the considered procedure of dynamic orbit determination. The basic data which were considered, are briefly described here. The detailed GRACE and GOCE data processing which is implemented here follows the standard procedures that are documented in the relevant literature (Papanikolaou and Tsoulis 2014; Papanikolaou 2012). For the case of GRACE, it incorporates the corrections to the initial KBR observations (Case et al. 2010) as well as the use of precise calibration parameters for the accelerometers provided by the TU Delft thermosphere web server thermosphere.tudelft.nl (Doornbos et al. 2009; Helleputte et al. 2009). For the case of GOCE, one cycle per revolution (1-CPR) empirical parameters have been included in the orbit estimation algorithm according to the following equation for each coordinate direction

Table 2 Orbit parameterization. Summary of the satellite dynamics, models and data

Satellite	GOCE	GRACE-A/GRACE-B
Orbit arc length	1 day	
Date	28/05/2010	17/11/2009
Earth rotation	IERS Conventions 2010 (Petit and Luzum 2010)	
EOP	08 C04 (Bizouard and Gambis 2009)	
Integrator	Adams–Bashforth-Moulton	
	Gauss-Jackson	
	Gauss-Jackson (pc)	
	RKN7(6)-8	
	RKN6(4)-6FD	
Start Integrator	RKN7(6)-8	
Integration step	1–30 s	1–60 s
Observations	Kinematic positions	Dynamic positions
Gravity model (d/o) (Mayer-Gürr et al. 2012)	GOCO03 s (150 × 150)	GOCO03 s (120 × 120)
Planetary ephemeris (Standish 1998)	DE423	
Solid earth tides	IERS Conventions 2010	
Ocean tides	FES2004 (Lyard et al. 2006)	
Non-gravitational forces	Drag-free orbit	Accelerometry data
Relativistic effects	IERS Conventions 2010	
Empirical parameters	Bias (along and cross-track) 1-CPR (along and cross-track)	Bias (along and cross-track)
External control	Reduced-dynamic orbit data	K-band ranging data

$$\ddot{r}_{1-CPR} = A\cos(u) + B\sin(u), \tag{23}$$

where u is the satellite's argument of latitude, $\ddot{r}_{1-CPR}$ is the 1-CPR acceleration and A, B are the unknown parameters to be estimated for each component.

In the following, we refer to the Adams–Bashforth-Moulton and Gauss-Jackson methods by using the terms ABM, GJ and GJ-pc. The pc particle in GJ-pc denotes the Gauss-Jackson formula that is implemented based on the predictor–corrector approach.

In the case of GOCE, the drag-free orbit concept is implemented due to the existence of the drag-free control system. The remaining drag-free system residuals are treated here by estimating empirical accelerations such as bias and one cycle per revolution perturbations for the along-track and cross-track components. The available GOCE precise orbit data (Bock et al. 2011, 2014) include the kinematic orbit data (used here as observations) and the reduced-dynamic orbit data. The GOCE estimated dynamic orbits, based on the aforementioned orbit modelling and the use of kinematic orbit positions as observations, are then compared to the precise reduced-dynamic orbit data. This is considered as an external orbit comparison that is performed between different orbit modelling procedures. The corresponding results based on the implemented numerical integration methods, are shown in Fig. 3 and Table 3.

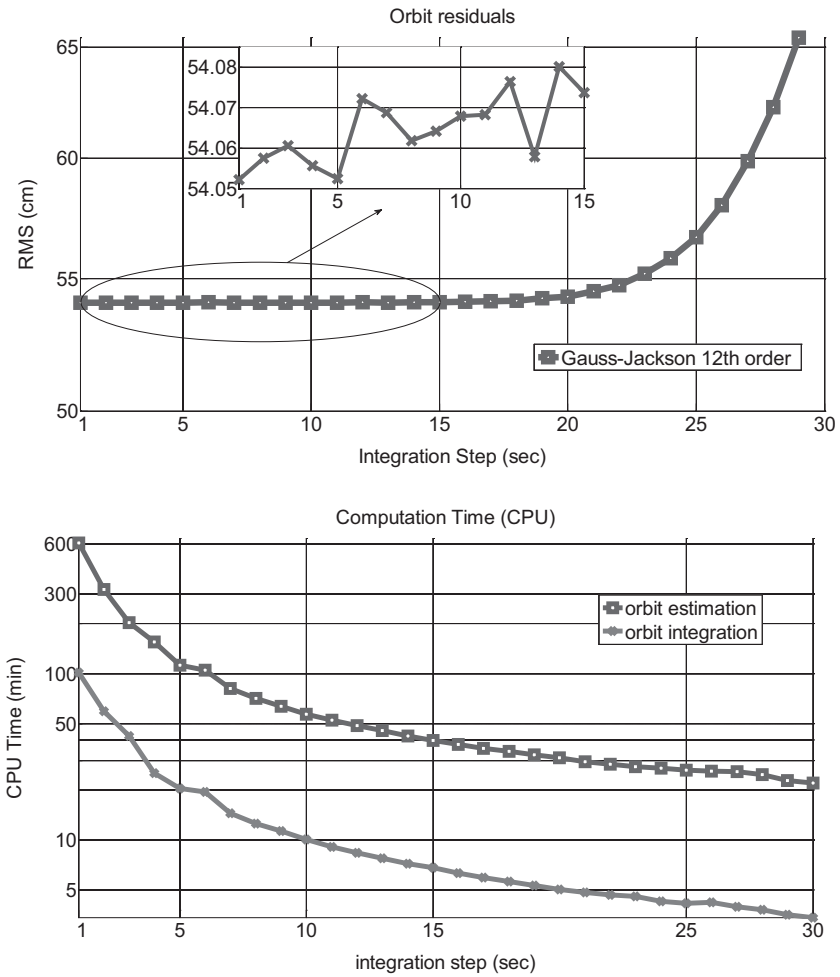

Fig. 3 RMS variances of GOCE orbit residuals based on the 12th order Gauss-Jackson method against the integration step in the range of 1–30 s. CPU time variations refer to the computation time that is required for the overall orbit estimation procedure and for the single orbit integration of the same arc

In the case of GRACE, dynamic orbit positions from the available precise orbit data (Case et al. 2010) have been used as observations in the orbit estimation procedure. Indeed, kinematic orbit positions would be identical for the current purpose, similarly to the implemented GOCE orbit analysis. Nevertheless, such kinematic orbit data of GRACE have not been available to the authors at the time of the performed computations. However, this discrepancy does not affect the present conclusions since these are mainly drawn according to the KBR analysis which forms an external validation of the orbits and the numerical integrators.

The non-gravitational effects of the GRACE satellites are computed based on the processing of the accelerometer data. In addition, during the orbit adjustment a bias acceleration is estimated for each of the along-track and cross-track directions.

Table 3 GOCE orbit residuals and external orbit comparison expressed by RMS in cm. The order of the multistep methods has been set equal to 12

Numerical integrators					
Step (s)	ABM	GJ	GJ-pc	RKN7(6)-8	RKN6(4)-6FD
Orbit residuals 3-D					
10	54.07	54.07	54.07	54.07	54.07
20	54.27	54.29	54.29	**54.06**	**54.06**
30	69.47	69.55	69.55	54.10	54.10
Orbit comparison: radial					
10	6.59	6.66	6.66	6.58	6.58
20	7.43	16.84	16.84	**6.57**	**6.57**
30	72.76	1074.19	1074.19	95.69	95.69
Orbit comparison: along-track					
10	59.19	**50.82**	**50.82**	60.05	60.05
20	59.61	866.36	866.35	62.24	62.24
30	5056.34	67,983.31	67,983.30	6943.23	6943.23
Orbit comparison: cross-track					
10	**23.63**	**23.63**	**23.63**	**23.63**	**23.63**
20	23.73	96.80	96.80	23.63	23.63
30	30.70	757.11	757.11	23.94	23.94
Overall computation (CPU) time (min)					
10	104	**55**	103	356	352
20	49	**29**	61	182	180
30	34	**21**	48	124	123

The bold values indicate the minimum values of the residuals

The GRACE mission implements the concept of low–low SST through an on-board microwave ranging system. The corresponding KBR observations may reach accuracy at the level of a few μm (Kim and Tapley 2002; Kang et al. 2006a) and therefore, such data analysis (Kang et al. 2006a, b) defines an external validation tool of the orbit modeling along the line-of-sight direction. The KBR data are not used as observations in the orbit estimation procedure and perform a relative control of the orbit accuracy. The critical parameter in KBR data analysis is the estimation of the unknown bias that is a characteristic of the range data. An alternative approach is also utilized which leads to the elimination of the KBR bias by forming range data differences between sequential epochs. The results of the GRACE orbit and KBR analysis based on variable parameters of the numerical integrators, are given in Figs. 4, 5, 6 and Tables 4, 5.

The computation time of the orbit determination has also been monitored in order to be considered as an additional criterion in the control test of the integrators' performance. The CPU time that has been recorded and is presented in the following tables, refers to calculations that have been carried out on a HP workstation (Intel Xeon 3.2 GHz). The overall computation time for each individual integration step, includes the time consumed by the integration of the equation of motion and the variational equations for all of the iterative steps of the orbit estimation algorithm.

In both cases, i.e. GOCE and GRACE satellites, an approach of pure dynamic orbit determination is implemented by adding only a few empirical parameters for treating the

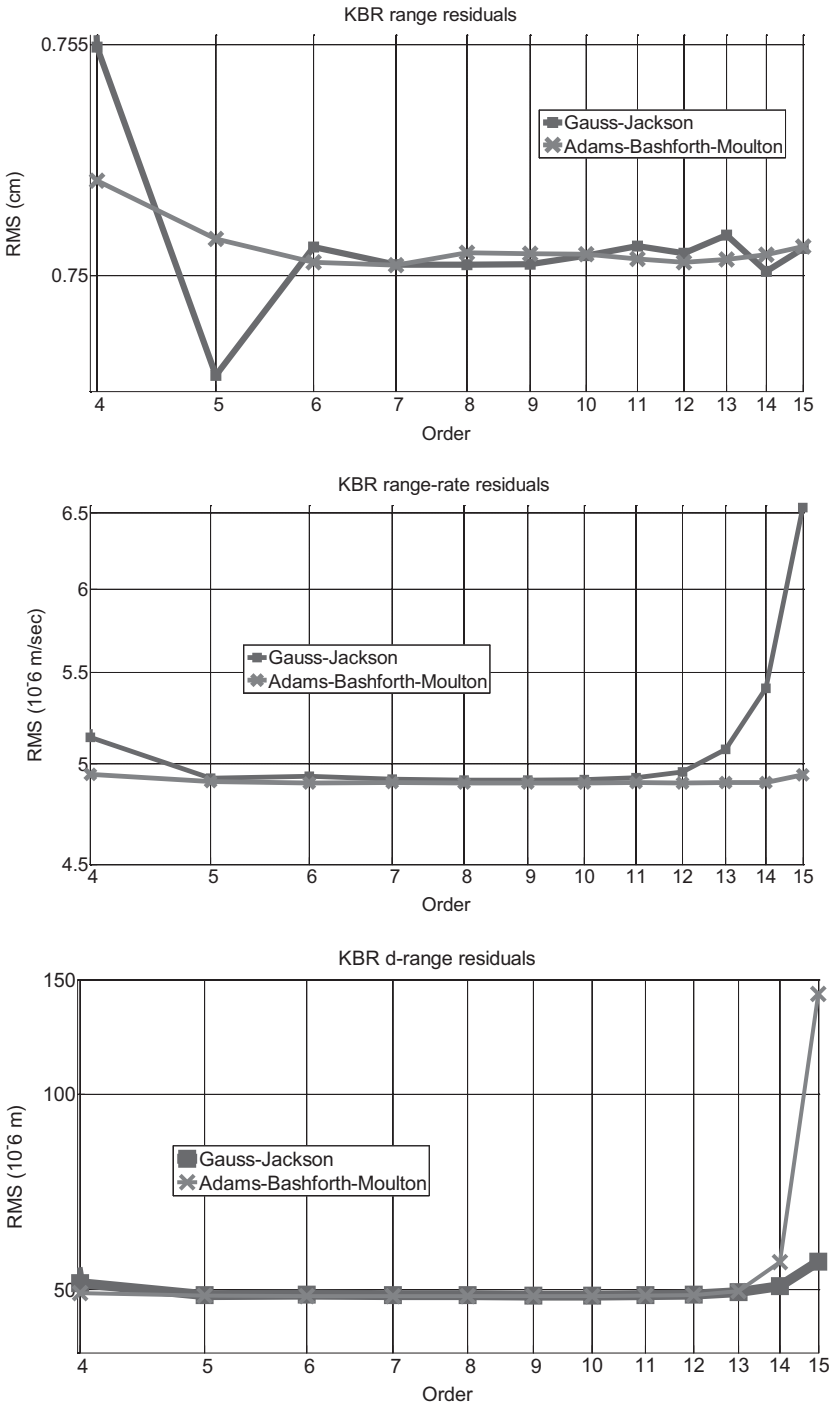

Fig. 4 RMS variances of KBR data residuals to the estimated GRACE dynamic orbits against the method's order. The term d-range refers to the approach of eliminating the KBR range bias based on sequential range differences

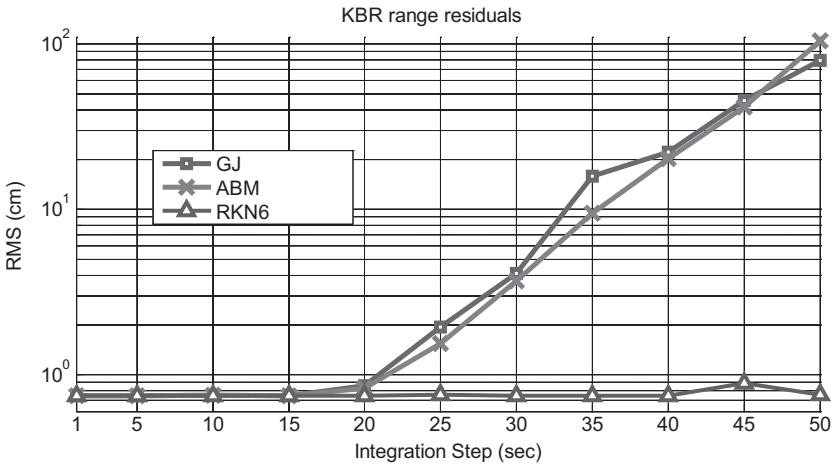
KBR range residuals
RMS (cm)
Integration Step (sec)
GJ
ABM
RKN6

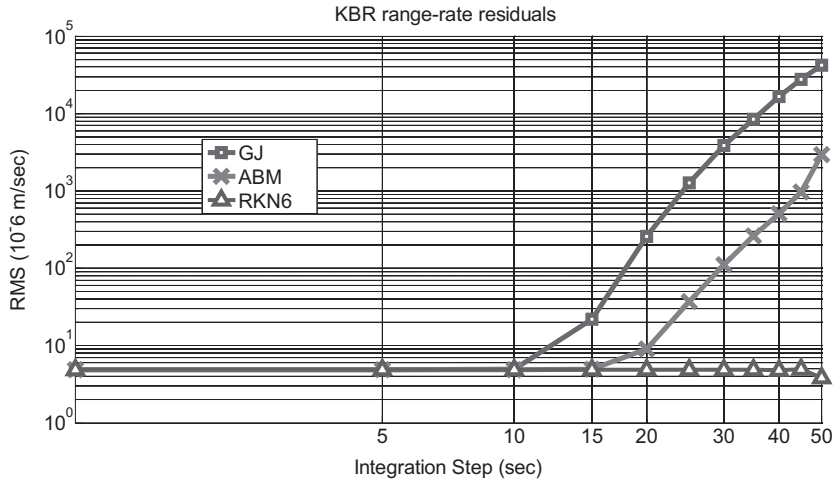
KBR range-rate residuals
RMS (10^-6 m/sec)
Integration Step (sec)
GJ
ABM
RKN6

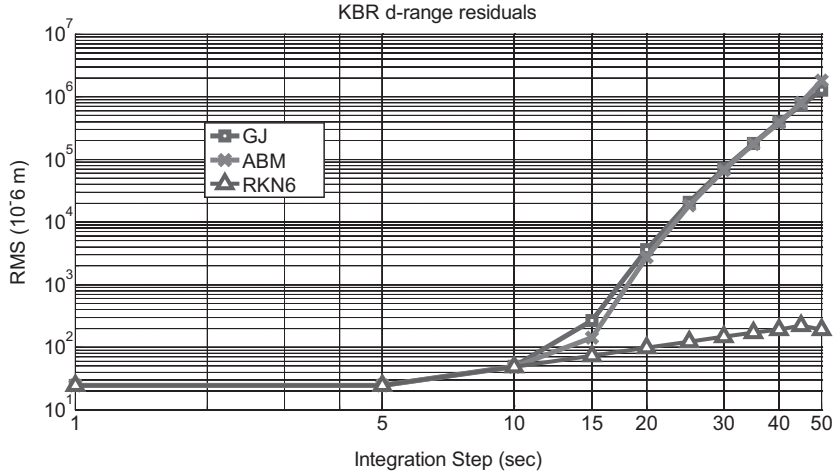
KBR d-range residuals
RMS (10^-6 m)
Integration Step (sec)
GJ
ABM
RKN6

◀**Fig. 5** RMS variances of KBR data residuals to the estimated GRACE dynamic orbits against the integration step in the range 1–50 s. The term d-range refers to the approach of eliminating the KBR range bias based on sequential range differences. The order of the multistep methods has been set equal to 12

non-gravitational effects. We avoid estimating several additional empirical accelerations which are widely used in precise orbit determination (Kang et al. 2006a; Jäggi et al. 2006; Montenbruck et al. 2005). Such parameterization leads to high accuracy, by means of orbit residuals, but may also absorb part of the errors that come from non-dynamic sources such as the numerical errors. The risk of such absorptions in the case of gravity field errors has been discussed by Zhu et al. (2004, 2003). Therefore, since the major scope in the present analysis is the assessment of the numerical integration methods through orbit analysis, we prefer to implement the scheme of pure dynamic orbit determination.

4.2 Results

The present GOCE and GRACE orbit analyses provide the means to derive an accuracy assessment of the implemented numerical integrators and make it possible to produce a comparison between them. The tools derived from the current analysis are based on the sophisticated observations techniques of the GOCE and GRACE missions.

In detail, the high density (rate 1 s) and quality of the kinematic orbit positions of the GOCE mission that are applied as observations in dynamic orbit determination, permit the step-wise analysis with interval of 1 s in order to control the variations in the full range of values for the integration's step size. Based on the estimated orbit residuals, the small values of the integration step i.e. lower than 10 s, has an effect at the level of few 10^{-4} m as it is illustrated in Fig. 3.

The KBR data analysis has been applied here as an external control of the orbit integrators accuracy. The KBR data are provided with a rate of 5 s and the conducted analysis with changing step size reveals sensitivity even at the values of the integration step lower than 10 s as it is shown in Table 5. Nevertheless, the GRACE orbit analysis does not show similar sensitivity at this range of the integration step but it may capture differences over the value of 20 s (Fig. 6).

Furthermore, GRACE orbit analysis has been also performed by reducing the integration step at 0.5 s. The respective computations have been applied for the Adams–Bashforth-Moulton and Gauss-Jackson methods. The Runge–Kutta–Nyström methods have been excluded since these methods are time-consuming and therefore, such integrators are not preferred for such low values of the integration step. The KBR residuals for setting integration step at 0.5, 1 and 5 s are given in Table 5. As it is shown, the KBR range residuals based on the sequential differences, decrease significantly for integration step lower or even equal to 5 s. However, CPU time increases dramatically for values lower than 5 s.

The applied approach of the step-wise orbit analysis reveals the variations and even the small discrepancies over the lower values of the integration step (<5 s). The orbit estimation algorithm has been repeated by modifying only the parameter of the integration step with an interval of 1 and 5 s for GOCE and GRACE respectively.

The order of the multistep methods has been tested in the range of 3–16. Over this limit the integration errors deteriorate the orbit accuracy by several orders of magnitude. The KBR analysis has shown acceptable precision for order values varying from 8 to 12 as it is drawn in Fig. 4. Similar results have been derived from GOCE orbit analysis which can be found in Fig. 3.

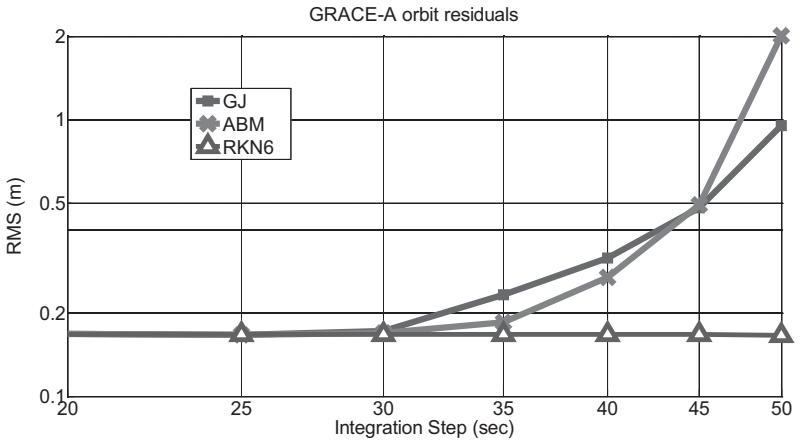
GRACE-A orbit residuals
GJ
ABM
RKN6
RMS (m)
Integration Step (sec)

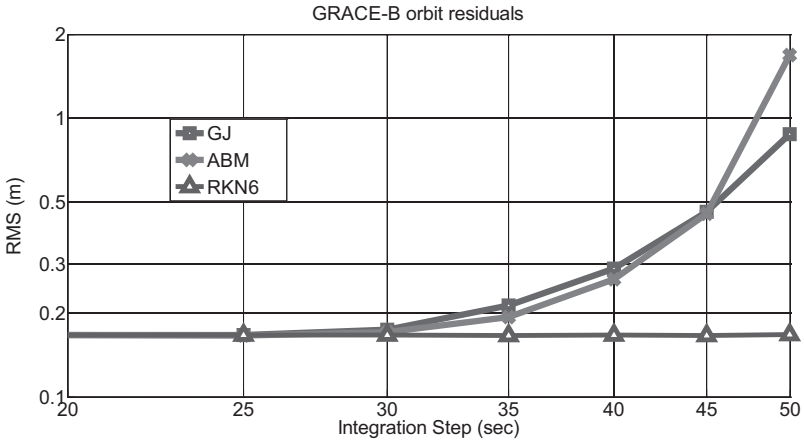
GRACE-B orbit residuals
GJ
ABM
RKN6
RMS (m)
Integration Step (sec)

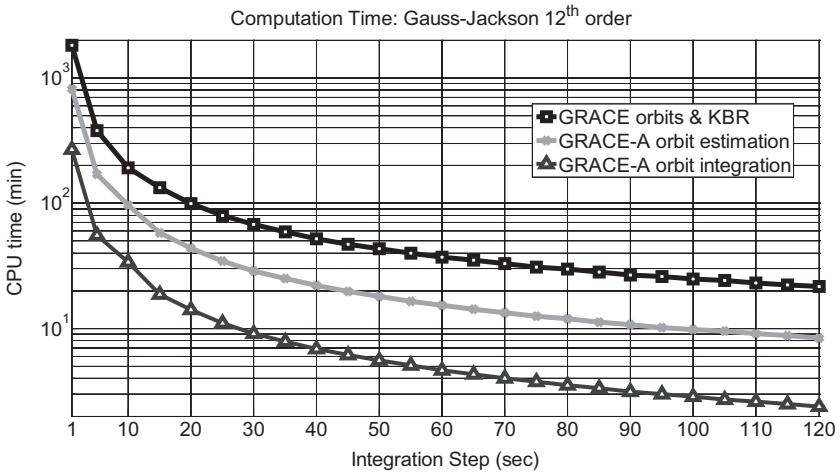
Computation Time: Gauss-Jackson 12th order
GRACE orbits & KBR
GRACE-A orbit estimation
GRACE-A orbit integration
CPU time (min)
Integration Step (sec)

◀**Fig. 6** RMS variances of GRACE orbit residuals against the integration step. The order of the multistep methods has been set equal to 12. CPU time variations refer to the computation time based on the Gauss-Jackson method. The CPU time is monitored for the overall procedure of GRACE orbits estimation and KBR analysis, the GRACE-A orbit estimation and the single orbit integration of the same arc. The order of the multistep methods has been set equal to 12

Table 4 K-band ranging data residuals of GRACE dynamic orbit determination. The order of the multistep methods has been set equal to 12

Numerical integrators					
Step (s)	ABM	GJ	GJ-pc	RKN7(6)-8	RKN6(4)-6FD
Range residuals: RMS (cm)					
10	0.7503	0.7505	0.7504	**0.7490**	0.7493
20	0.8311	0.8602	0.8604	**0.7491**	0.7498
30	3.6883	4.0877	4.0876	**0.7482**	0.7483
Range residuals (sequential-differences): RMS (μm)					
10	49.063	49.134	49.135	48.909	**48.907**
20	2721.287	3629.254	3629.254	97.708	97.880
30	66,656.183	71,675.319	71,675.319	146.487	147.163
Range-rate residuals: RMS (μm/s)					
10	4.9012	4.9560	4.9561	**4.9006**	4.9004
20	9.0259	256.9497	256.9497	**4.8931**	4.9017
30	111.8146	3854.4821	3854.4821	**4.8916**	4.9141
Overall computation (CPU) time (min)					
10	357	**192**	356	1971	1340
20	185	**99**	197	746	510
30	124	**68**	125	511	342

The bold values indicate the minimum values of the residuals

The performance of all numerical methods, implemented in the present analysis, remains at an equivalent level for step values up to 10 s. The Runge–Kutta–Nyström methods show high numerical stability in all cases, similarly with their behaviour in the Keplerian orbit analysis as it has been discussed in Sect. 3. In particular, this is mainly pronounced in Figs. 5 and 6, where the RKN6(4)-6FD method leads to stable residuals of GRACE orbit and KBR analysis for the overall integration step's range. On the other hand, the RKN methods are time consuming based on the current computations and thus they are not recommended in practice for such orbit determination problems. However, such problems dealing with computational effort can be treated based on parallel and modern GPU-accelerated computing techniques. Among the multistep methods, the Adams–Bashforth-Moulton method provides the highest accuracy, by means of orbit residuals, while the Gauss-Jackson requires the minimum CPU time.

It should also be remarked that significant orbit residuals are occurred in the case of the GOCE mission (Table 3). These residuals point to strong along-track perturbations and imply the existence of systematic effects which require further investigation. Certainly, these effects can be reduced through rigorous processing of the GOCE accelerometry data i.e. the common-mode accelerometers data, which capture the drag-free system residuals.

Table 5 K-band ranging data residuals for small values of the integration step. The order of the numerical integrators has been set equal to 12

Numerical integrators		
Step (s)	ABM	GJ
Range residuals: RMS (cm)		
0.5	0.7493	0.7494
1	0.7495	0.7487
5	0.7493	0.7486
Range residuals (sequential-differences): RMS (μm)		
0.5	24.4879	24.4883
1	24.4879	24.4884
5	24.4878	24.4889
Range-rate residuals: RMS (μm/s)		
0.5	4.90233	4.90242
1	4.90234	4.90244
5	4.90231	4.90255
Overall computation (CPU) time (min)		
0.5	7061	3887
1	3529	1823
5	701	380

This effort is still part of our on-going work and thus, it has not been taken into consideration in the present analysis. However, such an orbit improvement, expected to reach the level of 10^{-2} m, does not affect the present conclusions since these are based on the relative comparison of the numerical integration methods.

5 Summary and concluding remarks

The present study provides valuable assessment tools of the numerical integration methods for orbit determination of artificial satellites. In particular, the investigation is oriented especially to orbit modelling for LEOs. Two main approaches have been implemented in the adapted problem tests for the current purpose.

The classical test of the Keplerian orbit analysis, by performing the comparison between the analytical and numerical orbit integration, has been applied for the cases of LEO and MEO orbit types. However, since the integrators are affected by the satellite dynamics and the variety of the orbital characteristics, a realistic behavior of the numerical integrators has been revealed through the implemented dynamic orbit determination of LEOs i.e. GRACE and GOCE satellite orbit analysis.

The advantages from such a dynamic orbit analysis have been derived from the rigorous analysis of GRACE and GOCE orbital data. It has been shown that the KBR data together with the GOCE low orbit analysis are valuable tools for the accuracy assessment of numerical integration methods.

Moreover, the KBR space-borne observations, due to their high precision at micrometer level, present high sensitivity in the step-wise analysis of the integrators. The KBR data analysis has been demonstrated for integration stepsize at small values even down to 0.5 s.

Among the issues to be undertaken in the frame of our future work, we should mention the further modelling of the GOCE drag-free system residuals by processing of the GOCE common-mode accelerations.

Acknowledgments The authors acknowledge the European Space Agency for providing GOCE data, the Geoforschungszentrum Potsdam (GFZ-Potsdam) for providing the GRACE data, the Earth Orientation Center for providing the EOP data, JPL for providing the DE data and DEOS at TU Delft for providing the GRACE accelerometry calibration parameters. The motivation for the present work has emerged in the frame of European Space Agency Contract 22319/09/NL/CB.

References

Berry MM, Healy LM (2004) Implementation of Gauss-Jackson integration for orbit propagation. J Astronaut Sci 52(3):331–357

Beutler G (2005) Methods of celestial mechanics Vol. I: physical, mathematical and numerical principles. Springer, Berlin

Beutler G, Jäggi A, Mervart L, Meyer U (2010a) The celestial mechanics approach: application to data of the GRACE mission. J Geod 84(11):661–681

Beutler G, Jäggi A, Mervart L, Meyer U (2010b) The celestial mechanics approach: theoretical foundations. J Geod 85(10):605–624

Bizouard Ch, Gambis D (2009) The combined solution C04 for earth orientation parameters consistent with international terrestrial reference frame 2005. In: Drewes H (ed) Geodetic reference frames, IAG symposia series, vol 134. Springer, Berlin, pp 265–270

Bobojć A, Drożyner A (2003) Satellite orbit determination using satellite gravity gradiometry observations in GOCE mission perspective. Adv Geosci 1:1–4

Bock H, Jäggi A, Meyer U, Visser P, van de Ijssel J, van Helleputte T, Heinze M, Hugentobler U (2011) GPS-derived orbits for the GOCE satellite. J Geod 85(11):807–919

Bock H, Jäggi A, Beutler G, Meyer U (2014) GOCE: precise orbit determination for the entire mission. J Geod 88:1047–1060

Brouwer D (1959) Solution of the artificial satellite problem without drag. Astron J 64:378–397

Case K, Kruizinga G, Wu S (2010) GRACE level 1B data product user handbook. JPL Publication D-22027, version 1.3. Jet Propulsion Laboratory, California Institute of Technology

Casotto S (1993) Position and velocity perturbations in the orbital frame in terms of classical elements perturbations. Celest Mech Dyn Astron 55:209–221

Colombo OL (1986) Ephemeris errors of GPS satellites. Bull Géod 60:64–84

Cui C (1997) Satellite orbit integration based on canonical transformations with special regard to the resonance and coupling effects. Deutsche Geodätische Kommission, Reihe A, Heft Nr.112, München

Cui Ch, Lelgemann D (1995) Analytical dynamic orbit improvement for the evaluation of geodetic-geodynamic satellite data. J Geod 70:83–97

Cui Ch, Lelgemann D (2000) On non-linear low-low SST observation equations for the determination of the geopotential based on an analytical solution. J Geod 74:431–440

Doornbos E, Förster M, Fritsche B, van Helleputte T, van den Ijssel J, Koppenwallner G, Lühr H, Rees D, Visser P (2009) Air density models derived from multi-satellite drag observations, Final Report, ESA/ESTEC contract 21022/07/NL/HE, DEOS/TU Delft scientific report 01/2009

Dormand JR, Prince PJ (1978) New Runge-Kutta algorithms for numerical simulation in dynamical astronomy. Celest Mech Dyn Astron 18:223–232

Dormand JR, Prince PJ (1987) Runge-Kutta-Nystrom triples. Comput Math Appl 13(12):937–949

Elsaka B, Raimondo JC, Brieden P, Reubelt T, Kusche J, Flechtner F, Iran-Pour S, Sneeuw N (2014) Comparing seven candidate mission configurations for temporal gravity field retrieval through full-scale numerical simulation. J Geod 88(1):31–43

ESA (1999) Gravity field and steady-state ocean circulation mission, ESA SP-1233(1), Report for mission selection of the four candidate earth explorer missions. ESA Publications Division, ESTEC, Noordwijk

Floberghagen R, Fehringer M, Lamarre D, Muzi D, Frommknecht B, Steiger C, Pineiro J, da Costa A (2011) Mission design, operation and exploitation of the gravity field and steady-state ocean circulation explorer mission. J Geod 85:749–758

Förste Ch, Schmidt R, Stubenvoll R, Flechtner F, Ul Meyer, König R, Neumayer H, Biancale R, Lemoine J-M, Bruinsma S, Loyer S, Barthelmes F, Esselborn S (2008) The GeoForschungsZentrum Potsdam/

Groupe de Recherche de Gèodésie Spatiale satellite-only and combined gravity field models: EIGEN-GL04S1 and EIGEN-GL04C. J Geod 82:331–346
Fox K (1984) Numerical integration of the equations of motion of celestial mechanics. Celest Mech 33(2):127–142
Helleputte T, Doornbos E, Visser P (2009) CHAMP and GRACE accelerometer calibration by GPS-based orbit determination. Adv Space Res 43(12):1890–1896
Hull TE, Enright WH, Fellen BM, Sedgwick AE (1972) Comparing numerical methods for ordinary differential equations. SIAM J Numer Anal 9(4):603–637
Ilk KH, Löcher A, Mayer-Gürr T (2008) Do we need new gravity field recovery techniques for the new gravity field satellites? In: Xu PL, Liu JN, Dermanis A (eds) VI Hotine-Marussi symposium on theoretical and computational geodesy, International association of geodesy symposia, vol 132. Springer, Berlin, pp 3–8
Jäggi A, Hugentobler U, Beutler G (2006) Pseudo-stochastic orbit modelling techniques for low-earth orbiters. J Geodesy 80:47–60
Kang Z, Tapley B, Bettadpur S, Ries J, Nagel P, Pastor P (2006a) Precise orbit determination for the GRACE mission using only GPS data. J Geod 80:322–331
Kang Z, Tapley B, Bettadpur S, Ries J, Nagel P (2006b) Precise orbit determination for GRACE using accelerometer data. Adv Space Res 38:2131–2136
Kaula WM (1966) Theory of satellite geodesy. Dover Publication, Mineola
Kim J, Tapley BD (2002) Error analysis of a low-low satellite-to-satellite tracking mission. J Guid Control Dyn 25(6):1100–1106
Kozai Y (1959) The motion of a close earth satellite. Astron J 64:367–377
Loomis B, Nerem R, Luthcke S (2012) Simulation study of a follow-on gravity mission to GRACE. J Geod 86:319–335
Luthcke SB, Zelensky NP, Rowlands DD, Lemoine FG, Williams TA (2003) The 1-centimeter orbit: Jason-1 precision orbit determination using GPS, SLR, DORIS, and altimeter data. Mar Geod 26:399–421
Lyard F, Lefevre F, Letellier T, Francis O (2006) Modelling the global ocean tides: modern insights from FES2004. Ocean Dyn 56:394–415
Mayer-Guerr T et al. (2012) The new combined satellite only model GOCO03 s, Presented at GGHS2012, Venice
Montenbruck O (1992) Numerical integration methods for orbital motion. Celest Mech Dyn Astron 53:59–69
Montenbruck O, Gill E (2000) Satellite orbits; models, methods and applications. Springer, New York
Montenbruck O, van Helleputte T, Kroes R, Gill E (2005) Reduced dynamic orbit determination using GPS code and carrier measurements. Aerosp Sci Technol 9:261–271
Pail R, Bruinsma S, Migliaccio F, Forste C, Goiginger H, Schuh W-D, Hock E, Reguzzoni M, Brockmann JM, Abrikosov O, Veicherts M, Fecher T, Mayrhofer R, Krasbutter I, Sanso F, Tscherning CC (2011) First GOCE gravity field models derived by three different approaches. J Geod 85(11):819–843
Panet I, Flury J, Biancale R, Gruber T, Johannessen J, van den Broeke MR, van Dam T, Gegout P, Hughes CW, Ramillien G, Sasgen I, Seoane L, Thomas M (2013) Earth system mass transport mission (e.motion): a concept for future earth gravity field measurements from space. Surv Geophys 34(2):141–163
Papanikolaou TD (2012) Dynamic modelling of satellite orbits in the frame of contemporary satellite geodesy missions (in Greek), Ph.D. Dissertation, Aristotle University of Thessaloniki, Thesssaloniki
Papanikolaou TD, Tsoulis D (2014) Dynamic orbit parameterization and assessment in the frame of current GOCE gravity models. Phys Earth Planet Inter 236:1–9. doi:10.1016/j.pepi.2014.08.003
Petit G, Luzum B (2010) IERS Conventions 2010, IERS Technical Note No.36, Verlag des Bundesamts für Kartographie und Geodäsie, Frankfurt am Main
Seeber G (2003) Satellite geodesy, foundations, methods and applications. Walter de Gruyter, Berlin
Sheard BS, Heinzel G, Danzmann K, Shaddock DA, Klipstein WM, Folkner WM (2012) Intersatellite laser ranging instrument for the GRACE follow-on mission. J Geod 86:1083–1095. doi:10.1007/s00190-012-0566-3
Somodi B, Földvary L (2011) Application of numerical integration techniques for orbit determination of state-of-the-art LEO satellites. Period Polytech 55(2):99–106
Standish EM (1998) JPL planetary and lunar ephemerides; DE405/LE405, JPL IOM, 312F98-048
Svehla D, Rothacher M (2003) Kinematic and reduced-dynamic precise orbit determination of low Earth orbiters. Adv Geosci 1:47–56
Svehla D, Rothacher M (2005) Kinematic positioning of LEO and GPS satellites and IGS stations on the ground. Adv Space Res 36:376–381

Tapley BD, Bettadpur S, Watkins M, Reigber C (2004) The gravity recovery and climate experiment: mission overview and early results. Geophys Res Lett. doi:10.1029/2003GL019285

Tsoulis D, Ieronimaki Z, Kalampoukas G, Papanikolaou D, Papanikolaou T, Patlakis K, Vassiliadis I (2011) Spectral analysis and interpretation of current satellite-only Earth gravity models by incorporating global terrain and crustal data, Final Report, ESA Contract 22319/09/NL/CB

Wnuk E (1999) Recent progress in analytical orbit theories. Adv Space Res 23(4):677–687

Xu P (2008a) Position and velocity perturbations for the determination of geopotential from space geodetic measurements. Celest Mech Dyn Astron 100(3):231–249

Xu G (2008b) Orbits. Springer, Berlin

Zhu SY, Neumayer KH, Massmann F-H, Shi C, Reigber Ch (2003) Impact of different data combinations on the CHAMP orbit determination. In: Reigber Ch, Luehr H, Schwintzer P (eds) First CHAMP mission results for gravity, magnetic and atmospheric studies. Springer, Berlin, pp 92–97

Zhu S, Reigber Ch, König R (2004) Integrated adjustment of CHAMP, GRACE and GPS data. J Geod 78:103–108